SUPPLEMENTAL DATA

Supplemental Materials and Methods

GPCR profiling and validation

Experimental ONC212 GPCR profiling was performed utilizing the PathHunter beta-arrestin enzyme fragment complementation (EFC) assay at DiscoverX as described previously [1, 2]. PathHunter cells were seeded in a total volume of 20 µL into white walled, 384-well microplates and incubated at 37°C for the appropriate time prior to testing. For agonist determination, cells were incubated with ONC212 to induce response. 5 µL of 5x ONC212 was added to cells and incubated at 37°C or room temperature for 90 or 180 min. For antagonist determination, cells were preincubated with ONC212 followed by agonist challenge at the EC80 concentration (5 µL of 5x sample was added to cells and incubated at 37°C or room temperature for 30 min and 5 µL of 6x EC80 agonist in assay buffer was added to the cells and incubated at 37°C or room temperature for 90 or 180 min). Final assay vehicle concentration was 1%. Assay signal was generated through a single addition of 12.5 or 15 µL (50% v/v) of PathHunter Detection reagent cocktail, followed by 1-h incubation at room temperature. For some orphan GPCRs that exhibit low basal signal, activity was detected using a high sensitivity detection reagent (PathHunter Flash Kit) to improve assay performance. Microplates were read following signal generation with a PerkinElmer EnvisionTM instrument for chemiluminescent signal detection. Compound activity was analyzed using CBIS data analysis suite (ChemInnovation, CA). Initial screen against the GPCR panel was performed with 10 µM ONC212. For multi-dose validation, ONC212 was tested at concentrations from 1 nM up to 100 µM.

Genomics of Drug Sensitivity in Cancer (GDSC) cell line screening

Cell viability assays were performed as previously described [3-5] with 1,088 human cancer cell lines at 72 h post-ONC212 treatment to generate dose responses curves at concentrations from 78 nM up to 20 µM [4]. Cell viability was determined using either a DNA dye (Syto60) or metabolic assay (Resazurin or CellTitre-Glo). Fluorescence intensity data from screening plates for each dose response curve is fitted

using a multi-level fixed effect model [6] to generate GI50 and area under curve (AUC). We calculated AUC, instead of GI50, based on the dose response curves of each cell line, by which sensitivity of each cell line to ONC212 can be evaluated as continuous values with improved ability for comparisons. Also cell lines which were highly sensitive (< 78 nM) or highly resistant (> 20 μM) can be easily distinguished, which is not the case for GI50 values. ONC212 was broadly efficacious, in a nanomolar concentration range, against most solid and hematological malignancies.

The signaling profiling of GPR132

HEK293 cells were transfected in suspension with the human GPR132 receptor and one of the heterotrimeric G protein plasma membrane biosensors (Gαs, Gαi2, Gαz, Gαq, Gα14, Gα15/16, Gα12 or Gα13). These multimolecular BRET sensors detect the plasma membrane recruitment of proteins that interact with active Gα subunits in a G protein family-selective manner. Cells were maintained in DMEM supplemented with 1% penicillin-streptomycin and 10% FBS. At 48 h post transfection, cell were incubated with Tyrode-Hepes buffer (three different pH) for 60 min at 37 °C. Coelenterazine Prolume Purple (Nanolight, cat#369) was added to each well for a final concentration of 2 μM. ONC212 was added to each well and assayed at 22 concentrations with each biosensor. After 10 min incubation, BRET readings were collected with a 0.4 s integration time on a Synergy NEO plate reader (BioTek Instruments, Inc., Highland Park, IL; filters: 400 nm/70 nm, 515 nm/20 nm).

Establishment of gene knock-in cell lines

To establish GPR132 knock-out cell lines, we knocked in EF1α-GFP-T2A-Puro at the downstream of GPR132 start codon or AAVS1 locus. Gene knock-in cell lines were generated by MMEJ-assisted gene knock-in system using CRISPR/Cas9 with the PITCh systems [7]. The specific CRISPR target sequence (gagcaggatagtcctggtcg) designed for GPR132 and (attcccagggccggtta) for AAVS1 using CRISPRdirect (https://crispr.dbcls.jp/) were inserted in all-in-one CRISPR-Cas9 vector for CRIS-PITCh (v2) as previously described, [7] respectively. HR700PA-1 (MCS1-EF1α-GFP-T2A-Puro-pA-MCS2-PGK-

hsvTK; System Biosciences, CA, USA) was used for CRIS-PITCh(v2) vector [7] (HR700PA-1 PITCh GPR132/AAVS1). For GPR132, PITCh-gRNA target and 5' microhomology (MH) sequence (gcatcgtacgcgtacgtgtttggAGAGAGCAGGATAGTCCTGG) and 3' MH and PITCh-gRNA target sequence (TCGTGGTGTACAGCGCGGTGccaaacacgtacgcgtacgatgc) were inserted in MCS1 and MCS2 of HR700PA-1, respectively. For AAVS1, PITCh-gRNA target and 5' MH (gcatcgtacgcgtacgtgtttggTATATTCCCAGGGCCGGTTA) and 3' MH for GPR132 and PITCh-gRNA target sequence (ATGTGGCTCTGGTTCTGGGTccaaacacgtacgcgtacgatgc). Both vector were transfected into HCT-116 cells. Three days post-transfection, the transfected cells were cultured with 1 μg/ml of puromycin for 1 week, and then the cells were treated with 10 μg/ml of ganciclovir for 1 week. After puromycin and ganciclovir selection, we performed single cell cloning using FACSMelody cell sorter (BD Biosciences, CA, USA). Two weeks post-sorting, gene knock-in cell lines were confirmed by genotyping using genomic PCR and direct sequencing. Design of genomic PCR primers are shown in Supplemental Fig. 3. GPR132 Fw (primer 1); 5'-gactcccgtcctcactcttg-3', GPR132 Rv (primer 2); 5'-agatgtaggcggtcaccttg-3', HR700PA-1 Rv (primer 3); 5'-ccttctctaggcacccgttc-3', HR700PA-1 Fw (primer 4); 5'-gggaggattgggaagagaata-3', AAVS1 Fw; 5'-cccctatgtccacttcagga-3', and AAVS1 Rv; 5'-cctctctggctccatcgtaa-3'.

Quantitative reverse transcription polymerase chain reaction (qRT-PCR)

qRT-PCR was carried out using the TaqMan Fast Advanced Master Mix (Thermo Fisher Scientific, San Jose, CA, USA), the 7900HT Fast Real Time PCR System (Thermo Fisher Scientific), and the TaqMan Gene Expression Assays listed in Supplemental Table 1. GAPDH was used as an internal control.

Immunoblot analysis

Cells were incubated on ice with cell lysis buffer containing protease/phosphatase inhibitor cocktail (Cell Signaling Technology, Beverly, MA, USA). The cell lysates were then resolved by SDS-polyacrylamide gel electrophoresis, followed by immunoblotting. As to GPR132 detection, we collect the membrane fraction as previously described [8]. The primary antibodies used are shown in Supplemental Table 1. The signals and band intensities were analyzed using the Odyssey Imaging System (LI-COR Biotechnology, Lincoln, NE, USA).

Subcutaneous xenograft experiment

AML subcutaneous xenograft studies in athymic nude mice were performed at Noble Life Sciences. The study was conducted in compliance with the current version of the following: 1) Animal Welfare Act Regulations (9 CFR); 2) U.S. Public Health Service Office of Laboratory Animal Welfare (OLAW) Policy on Humane Care and Use of Laboratory Animals; 3) Guide for the Care and Use of Laboratory Animals (Institute of Laboratory Animal Resources, Commission on Life Sciences, National Research Council, 1996); and 4) AAALACi accreditation. All procedures were conducted under a protocol that was approved by Noble Life Sciences IACUC. Athymic nude mice (Envigo, 6- to 7-week-old female) were used. Cells (5 million cells per injection) were subcutaneously injected as a suspension (30% Matrigel in HBSS) into the right and left flank of the mice. ONC212 and ONC201 treatment was started when the tumors reached a detectable volume (~150 mm3). Mice were randomly assigned to groups, and administered vehicle (sterile injectable water) or ONC201 or ONC212 with oral gavage at indicated doses and intervals. Tumor growth and body weight was monitored until the endpoint. No blinding was used for the evaluations of the animal studies.

***Ex vivo/in vivo* engraftment experiments**

Ex vivo engraftment experiments were performed as previously reported [9]. Primary AML cells were transplanted into female NSG mice (6 wk old; Jackson Laboratory) to confirm self-renewal ability, and

leukemia cells were harvested from secondarily transplanted mice. Leukemic cells were cultured for 36 h, with or without 250 nM of ONC212, then washed and assessed for viability by Trypan blue exclusion; 0.7 million Trypan blue–negative cells were then injected via tail vein into each of female NSG mice per group. At one month after transplantation, human CD45-positive and DAPI-negative cells in peripheral blood were analyzed by flow cytometry, and three mice in each group were sacrificed to collect BM, spleens, and livers and used for flow cytometry. Human and mouse CD45-positive and DAPI-negative cells in the BM were analyzed by flow cytometry. The remaining 7 mice in each group were monitored for survival. The ex vivo mouse studies were performed following the guidelines approved by the Institutional Animal Care and Use Committee at MD Anderson Cancer Center.

In vivo ONC212 monotherapy and combination therapy with ABT-199

In vivo ONC212 monotherapy and combination therapies with ABT-199 were performed, with some modifications, as reported previously [10]. Female NSG-S mice were intravenously injected with luciferase-labeled OCI-AML3 cells (1.0×10^6 cells/mouse for monotherapy) or MOLM13 cells (0.7×10^6 cells/mouse for combination therapy) and evenly divided by body weight into four groups. For ONC212 monotherapy, seven d post injection, the mice were treated with vehicle, ONC212 (50 mg/kg body weight; twice a wk; oral gavage) until death. For ONC212 combination therapy with ABT-199, three d post injection, the mice were treated with vehicle, ONC212 (50 mg/kg body weight; three time per wk; oral gavage), ABT-199 (100 mg/kg body weight; daily; oral gavage) or combination of ONC212 and ABT-199 until death.

For oral dosing, ONC212 was formulated in water and ABT-199 was formulated in 60% phosal 50 propylene glycol, 30% polyethyleneglycol-400, and 10% ethanol. Bioluminescent imaging (BLI) was used to monitor tumor burden at different time points. Briefly, mice were anaesthetized and injected intraperitoneally with 100 μl of D-luciferin (40 mg/ml; Gold Biotechnology, MO, USA) and then imaged noninvasively using the IVIS-200 in vivo imaging system (PerkinElmer, MA, USA). One mouse (for

monotherapy, after 45 d) or three mice (for combination, after 14 d) from each group were sacrificed by CO2 asphyxiation. BM, spleens, and livers were collected for flow cytometry. The remaining mice in each group were followed for survival. The in vivo mouse study was performed following the guidelines approved by the Institutional Animal Care and Use Committees at MD Anderson Cancer Center.

References

1. Cohen LJ, Kang HS, Chu J, Huang YH, Gordon EA, Reddy BVB, Ternei MA, Craig JW, Brady SF. Functional metagenomic discovery of bacterial effectors in the human microbiome and isolation of commendamide, a GPCR G2A/132 agonist. Proceedings of the National Academy of Sciences of the United States of America. 2015; 112: E4825-E34. doi: 10.1073/pnas.1508737112.

2. Shehata MA, Belcik Christensen H, Isberg V, Sejer Pedersen D, Bender A, Bräuner-Osborne H, Gloriam DE. Identification of the first surrogate agonists for the G protein-coupled receptor GPR132. RSC Advances. 2015; 5: 48551-7. doi: 10.1039/c5ra04804d.

3. Garnett MJ, Edelman EJ, Heidorn SJ, Greenman CD, Dastur A, Lau KW, Greninger P, Thompson IR, Luo X, Soares J, Liu Q, Iorio F, Surdez D, et al. Systematic identification of genomic markers of drug sensitivity in cancer cells. Nature. 2012; 483: 570-5. doi: 10.1038/nature11005.

4. Wagner J, Kline CL, Ralff MD, Lev A, Lulla A, Zhou L, Olson GL, Nallaganchu BR, Benes CH, Allen JE, Prabhu VV, Stogniew M, Oster W, et al. Preclinical evaluation of the imipridone family, analogues of clinical stage anti-cancer small molecule ONC201, reveals potent anti-cancer effects of ONC212. Cell Cycle. 2017: 0. doi: 10.1080/15384101.2017.1325046.

5. Yang W, Soares J, Greninger P, Edelman EJ, Lightfoot H, Forbes S, Bindal N, Beare D, Smith JA, Thompson IR, Ramaswamy S, Futreal PA, Haber DA, et al. Genomics of Drug Sensitivity in Cancer (GDSC): a resource for therapeutic biomarker discovery in cancer cells. Nucleic Acids Res. 2013; 41: D955-61. doi: 10.1093/nar/gks1111.

6. Vis DJ, Bombardelli L, Lightfoot H, Iorio F, Garnett MJ, Wessels LF. Multilevel models improve precision and speed of IC50 estimates. Pharmacogenomics. 2016; 17: 691-700. doi: 10.2217/pgs.16.15.

7. Sakuma T, Nakade S, Sakane Y, Suzuki KT, Yamamoto T. MMEJ-assisted gene knock-in using TALENs and CRISPR-Cas9 with the PITCh systems. Nat Protoc. 2016; 11: 118-33. doi: 10.1038/nprot.2015.140.

8. Hattori T, Obinata H, Ogawa A, Kishi M, Tatei K, Ishikawa O, Izumi T. G2A plays proinflammatory roles in human keratinocytes under oxidative stress as a receptor for 9-hydroxyoctadecadienoic acid. J Invest Dermatol. 2008; 128: 1123-33. doi: 10.1038/sj.jid.5701172.

9. Ishizawa J, Kojima K, Chachad D, Ruvolo P, Ruvolo V, Jacamo RO, Borthakur G, Mu H, Zeng Z, Tabe Y, Allen JE, Wang Z, Ma W, et al. ATF4 induction through an atypical integrated stress response to ONC201 triggers p53-independent apoptosis in hematological malignancies. Sci Signal. 2016; 9: ra17. doi: 10.1126/scisignal.aac4380.

10. Pan R, Hogdal LJ, Benito JM, Bucci D, Han L, Borthakur G, Cortes J, DeAngelo DJ, Debose L, Mu H, Dohner H, Gaidzik VI, Galinsky I, et al. Selective BCL-2 inhibition by ABT-199 causes on-target cell death in acute myeloid leukemia. Cancer Discov. 2014; 4: 362-75. doi: 10.1158/2159-8290.cd-13-0609.

Taqman gene expression assays

Target gene	Assay ID of Taqman gene expression assays
GPR132	Hs00203431_m1
DDIT3 (CHOP)	Hs00358796_g1
TNFRSF10B (DR5)	Hs00169585_m1
GADD34	Hs00169585_m1
TRIB3	Hs01082394_m1
GAPDH	Hs02758991_g1

Antibodies for Western blotting

Target protein	Clone	Conpany
Phospho-eIF2a (Ser51)	E91	Abcam
eIF2α	FL-3115	Cell Signaling Technology
ATF4	D4B8	Cell Signaling Technology
p53	DO-1	Santa Cruz Biotechnology
α-tubulin	T8203	Sigma-Aldrich
MCL-1	S-19	Santa Cruz Biotechnology
BCL-XL	Polyclonal (#2762)	Cell Signaling Technology
BCL-2	N-19	Santa Cruz Biotechnology
GPR132	G-5	Santa Cruz Biotechnology
Na+ K+ ATPase	H-3	Santa Cruz Biotechnology
β-Actin	AC-74	Sigma-Aldrich

Supplemental table 1

	Karyotype	mutation
Patient-1	**49~53,XX,del(5)(q13q33),add(11)(q21),der(11)hsr(11)(q23), -13,+22,+der(?)r(11)hsr(11)(q23)x1-2,+der(?)ins(?;11)(?;q23q23)x2-5,+1-2mar[cp20]. FISH positive for del 5q31 and amplification (but not rearrangement) of KMT2A**	**TP53 A161T, R213L, DNMT3A E774G. This one probably germline: KIT M541L**
Patient-2	**49,XY,del(5)(q22q35),+6,+8,der(11)t(5;11)(q22;q25), +13,-14,+15,der(15;17)(q10;q10)x2,+17,+22,6-11dmin[cp20]. FISH positive for KMT2A amplification, deletion of TP53 gene, gain of extra copy of chromosome 17, and gain of extra copy of MYC.**	**TP53 C238Y, This one probably of germline origin: IDH1 V178I.**
Patient-3	**43,X,add(X)(p22.1),del(5)(q22q35),-16,-17,-18[7]/43,idem,der(11)t(11;11)(p14;q12)[1]/57,XX,+1,+2,+del(5)(q22q35),+6,+8,+9,+10,+11,der(11)t(11;11)(p14;q12),+14,+15,+22[12]**	**TP53 R248Q, D259V, IDH2 R140Q, PTPN11 E69K, DNMT3A G543D.**

Supplemental table 2

Supplemental Table 3 ONC212 multi-dose validation of Top 6 GPCRs

Compound Name	Assay Name	Assay Format	Assay Target	Result Type	RC50 (uM)	Hill	Curve Bottom	Curve Top	Max Response
CCL22	Arrestin	Agonist	CCR4	EC50	0.002317715	0.74493	0	103.71	101.68
C 021 dihydrochloride	Arrestin	Antagonist	CCR4	IC50	0.004555436	0.77513	0	100.88	100.95
Acetylcholine	Arrestin	Agonist	CHRM2	EC50	11.14243	1.0339	-1.1491	101.93	102.15
Atropine	Arrestin	Antagonist	CHRM2	IC50	0.007830328	1.1132	-0.94034	101.5	100.49
Melanotan II	Arrestin	Agonist	MC4R	EC50	0.000710297	1.0927	-1.3001	99.9	101.13
HS024	Arrestin	Antagonist	MC4R	IC50	0.00085552	0.95916	0	98.16	101.81
ONC212	Arrestin Orphan	Agonist	BAI3	EC50	>100				191.38
ONC212	Arrestin	Antagonist	CCR4	IC50	17.48115	1.6992	0	99.717	94.915
ONC212	Arrestin	Antagonist	CHRM2	IC50	>100				8.8533
ONC212	**Arrestin Orphan**	**Agonist**	**GPR132**	**EC50**	**0.4051399**	**2.2025**	**4.9512**	**195.93**	**194.83**
ONC212	Arrestin Orphan	Agonist	GPR162	EC50	>100				30.811
ONC212	Arrestin	Antagonist	MC4R	IC50	28.56012	0.89197	-1.4776	86.454	63.63

ONC212 multi-dose validation using the PathHunter β-Arrestin assay for top 6 hits identified in the GPCR screen. ONC212 was tested at concentrations from 1 nM up to 100 µM. Results presented as EC50/IC50.

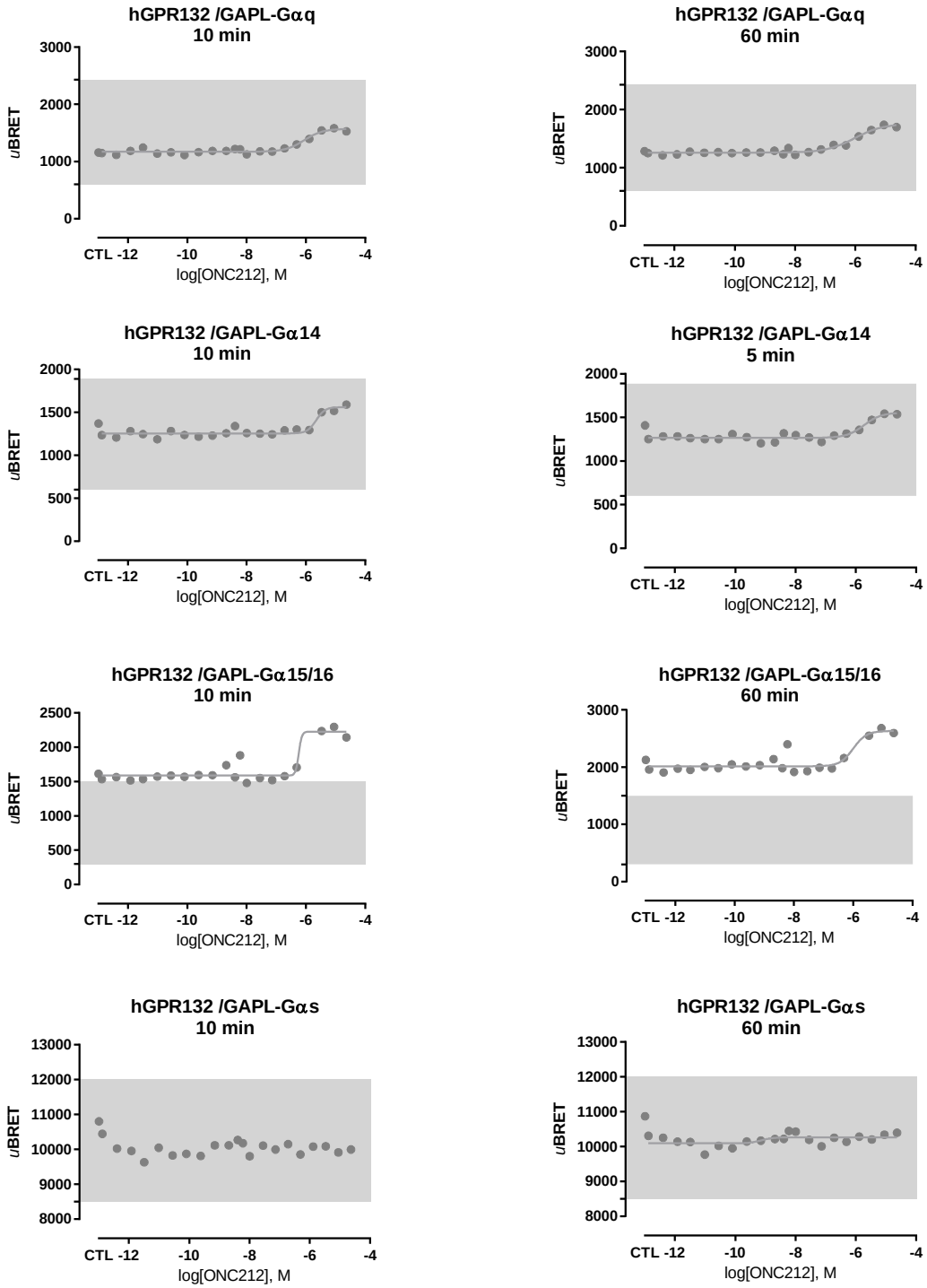

Supplemental Figure 1. Effects of ONC212 on various subtype-specific Gα-protein activation biosensors
HEK293 were co-transfected with 200 ng of plasmid encoding hGPR132-FLAG tag and plasmids coding for the GAPL-Gαq,GAPL-Gα14, GAPL-Gα15/16 or GAPL-Gαs biosensor. Increasing amounts of ONC212 were added and the BRET assay was performed as described in Materials and Methods. Experimental data were produced in singleton and curves were fitted using the 4-parameter logistic non-linear regression model (GraphPad 6). Data in graphs represent a 5, 10 or 60 minute incubation with ONC212 and expressed as uBRET.

Supplemental Figure 1

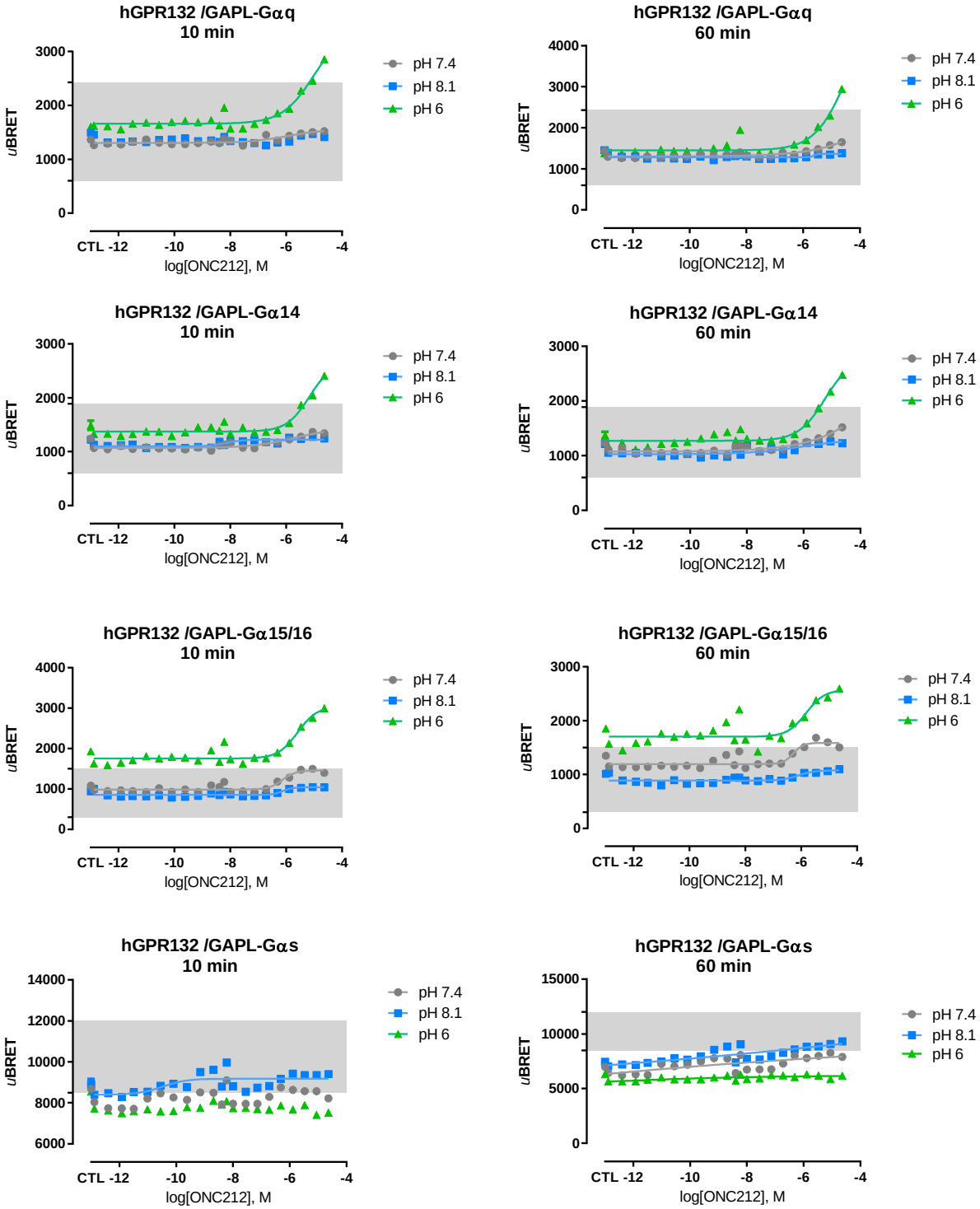

Supplemental Figure 2. Effects of ONC212 on various subtype-specific Gα-protein activation biosensors
HEK293 were co-transfected with 200 ng of plasmid encoding hGPR132-FLAG tag and plasmids coding for the GAPL-Gαq,GAPL-Gα14, GAPL-Gα15/16 or GAPL-Gαs biosensor. Increasing amounts of ONC212 were added and the BRET assay was performed at the indicated levels of pH. Experimental data were produced in singleton and curves were fitted using the 4-parameter logistic non-linear regression model (GraphPad 6). Data in graphs represent a 5, 10 or 60 minute incubation with ONC212 and expressed as uBRET.

Supplemental Figure 2

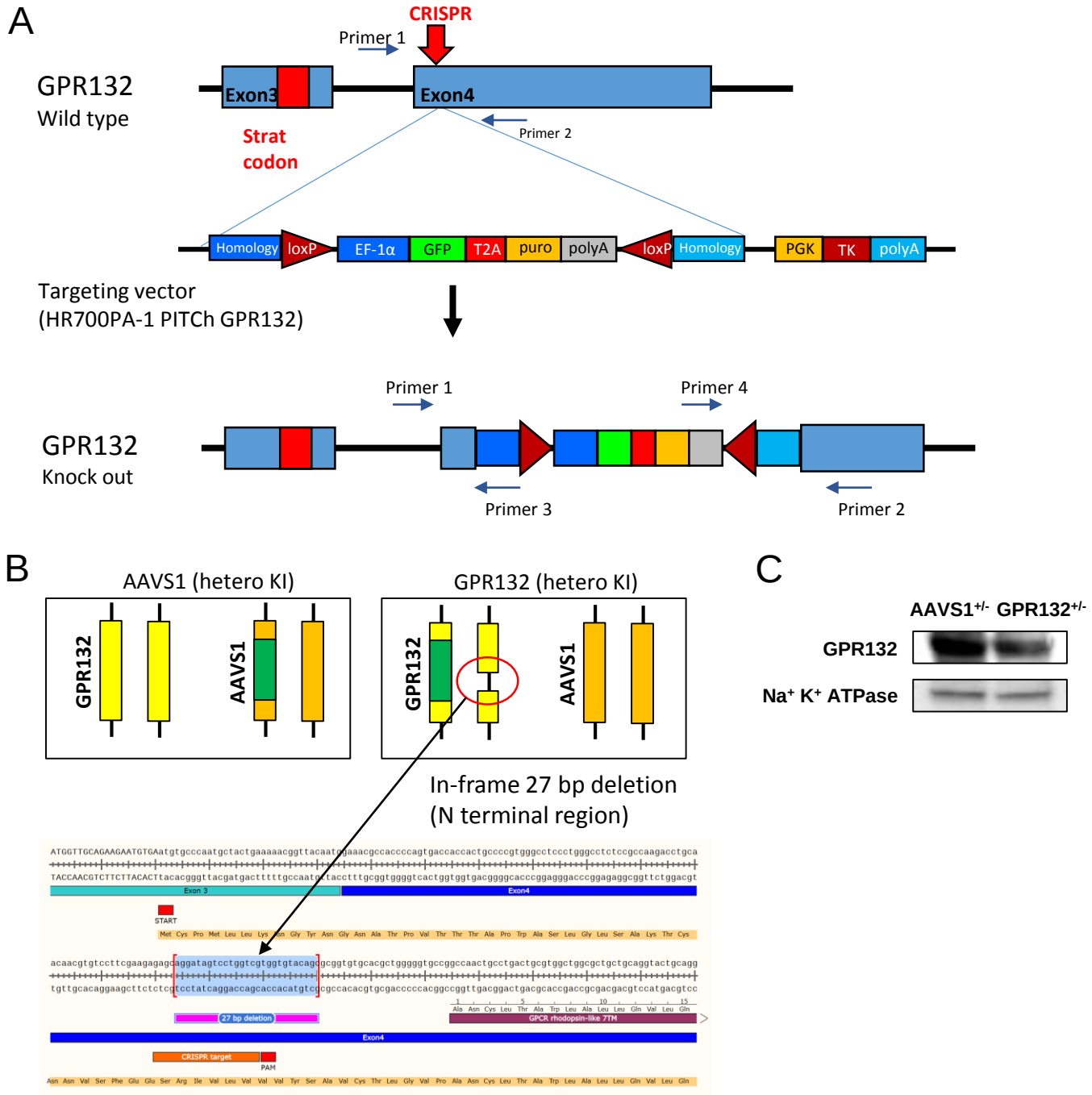

Supplemental Figure 3. Vector construction for CRIS-PITCh (v2)–mediated gene knock-in. (A) Illustrations of wild-type, targeting vector, and knock-out alleles. (B) Genomic sequence of GPR132 gene. heterozygous knock-out clone has knock-in allele and in-frame 27 base-pair deletion on the other allele. (C) Western blotting analysis of GPR132 expression. Na^+ K^+ ATPase was used as a loading control of membrane fraction of the cells.

Supplemental Figure 3

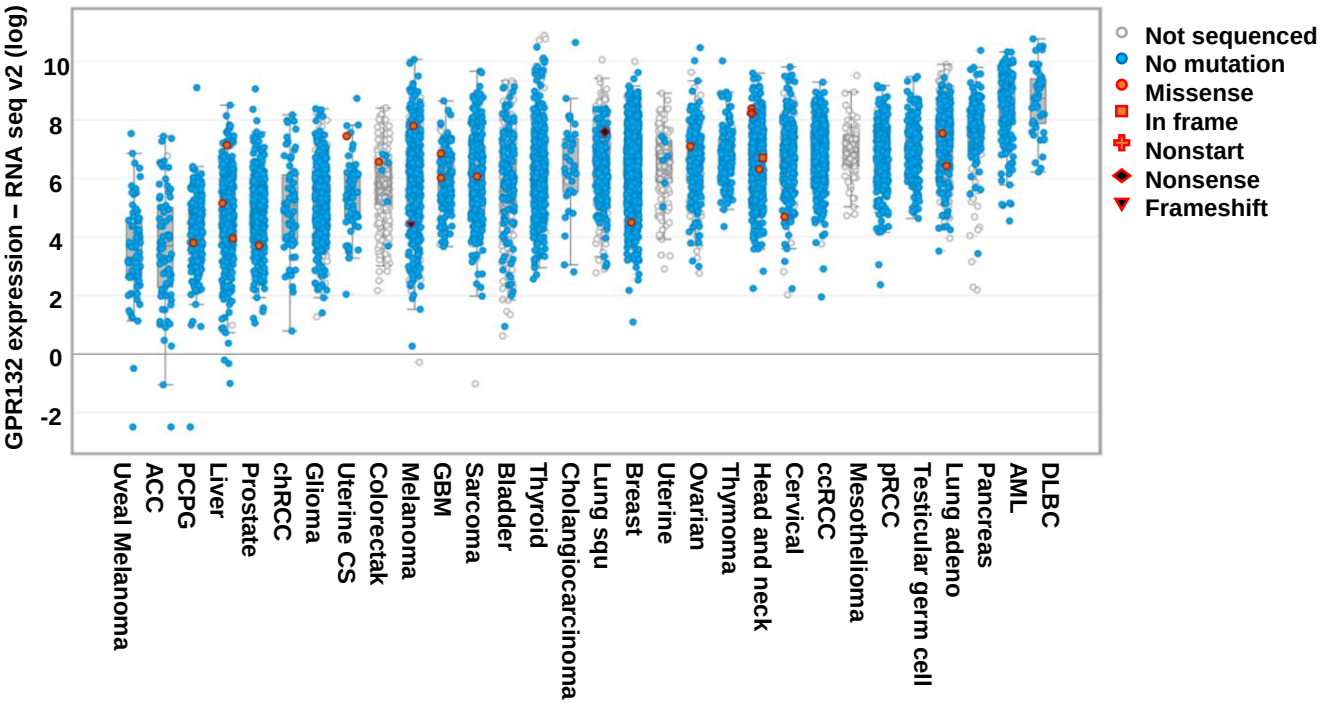

Supplemental Figure 4. ONC212 increases orphan GPCR GPR132 expression.
GPR132 expression analysis of samples in the Cancer Genome Atlas (TCGA) analyzed by cBioPortal.

Supplemental Figure 4

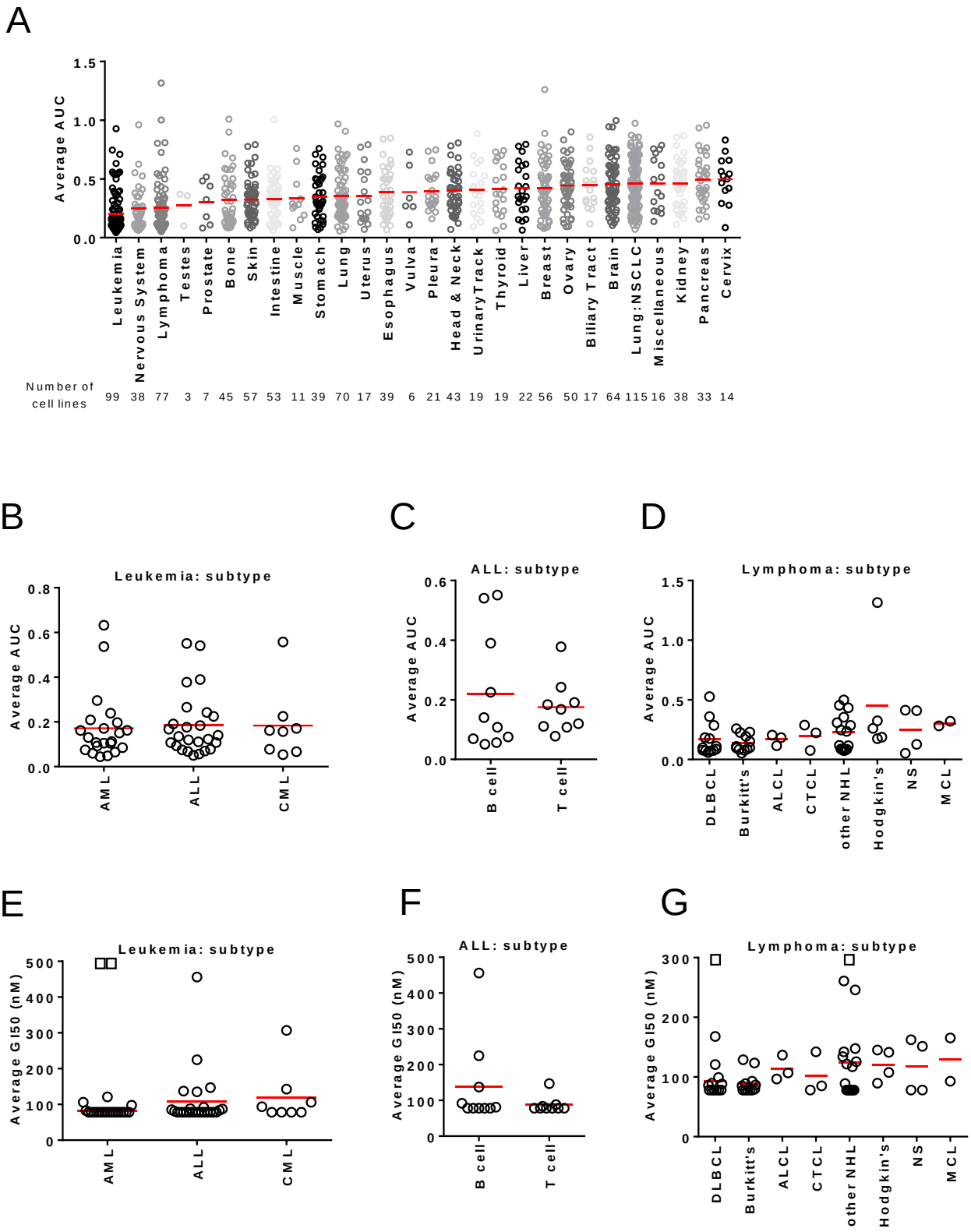

Supplemental Figure 5

Supplemental Figure 5. ONC212 anti-tumor effects on leukemia and lymphoma. (A) *In vitro* sensitivity of 1088 human cancer cell lines to ONC212 (78 nM - 20 μM, 72 h) organized by tumor type. The results are shown as average ONC212 area under the dose response curve (AUC) with representation of all cell lines in each tumor type. The number of cell lines tested per tumor type are indicated. (B) AUC for AML (n = 22), ALL (n = 25) and CML (n = 8) cell lines treated with ONC212 (78 nM - 20 μM, 72h) in the GDSC screen. ONC212 demonstrated broad spectrum anti-leukemic activity. (C) AUC for B cell ALL (n = 10) and T cell ALL (n = 9) cell lines treated with ONC212 (78 nM – 20 μM, 72hr) in the GDSC screen. Both B-cell and T-cell ALL were highly sensitive to ONC212. (D) AUC for DLBCL (n = 13), Burkitt's (n = 12), Anaplastic large cell (ALCL; n = 3), CTCL (n = 3), other NHL (n = 15), other Hodgkins lymphoma (HL; n = 5), nodular sclerosis (NS; n = 4) and MCL (n = 2) cell lines treated with ONC212 (78 nM – 20 μM, 72 h) in the GDSC screen. ONC212 showed broad spectrum anti-lymphoma activity. (E) GI50 (nM) for AML (n = 22), ALL (n = 25) and CML (n = 8) cell lines treated with ONC212 (78 nM - 20 μM, 72h) in the GDSC screen. Two AML cell lines were unresponsive (GI50 > 20 μM) and showed in square. (F) GI50 (nM) for B-cell ALL (n = 10) and T-cell ALL (n = 9) cell lines treated with ONC212 (78 nM - 20 μM, 72h) in the GDSC screen. Both B-cell and T-cell ALL were highly sensitive to ONC212. (G) GI50 (nM) for DLBCL (n = 13), Burkitt's (n = 12), Anaplastic large cell (ALCL; n = 3), CTCL (n = 3), other NHL (n = 15), other Hodgkins lymphoma (HL; n = 5), nodular sclerosis (n = 4) and MCL (n = 2) cell lines treated with ONC212 (78 nM - 20 μM, 72 h) in the GDSC screen. Two cell lines (DLBCL and other HL) were unresponsive and (GI50 > 20 μM) and showed in square. ONC212 showed broad spectrum anti-lymphoma activity. Most of the leukemia cell lines (i.e., 53 of 55) were responsive to ONC212 with a GI50 ranging from < 78 nM to 456 nM. Among ALL lines, both B-cell and T-cell ALL were highly sensitive to ONC212 (B and E). ONC212 reduced cell viability in most lymphoma lines (i.e., 55 of 57) and was equally efficacious regardless of subtypes with GI50 values ranging from < 78 nM to 261 nM (C and F).

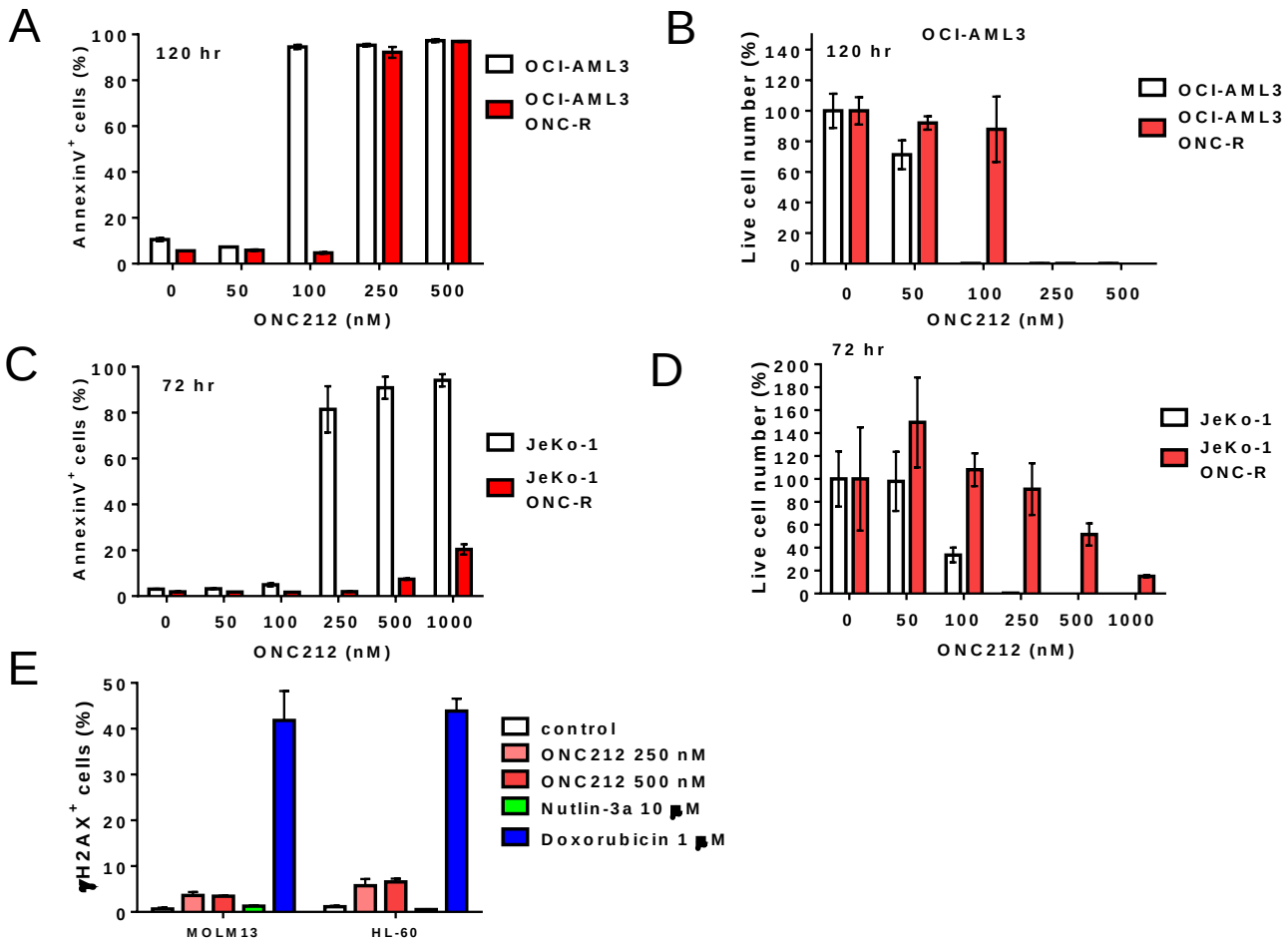

Supplemental Figure 6. Cross resistance to ONC212 with ONC201 in AML and MCL cell lines.
(A) The percentage of apoptotic cells (annexinV+ cells) induced by ONC212 treatment for 120 h in parental or ONC201-resistant (ONC-R) OCI-AML3 cells. (B) The percentage of live cell numbers after a 120 h-treatment with ONC212 in parental or ONC-R OCI-AML3 cell. (C) The percentage of apoptotic cells induced by ONC212 treatment for 72 h in parental or ONC-R JeKo-1 cell line. (D) The percentage of live cell numbers after a 72 h-treatment with ONC212 in parental or ONC-R JeKo-1cell line. (E) Flow cytometric analysis of γH2AX positive cells in MOLM13 and HL-60 cells treated with ONC212, Nutlin-3a, and Doxorubicin for 24 h. Data are shown as the mean ± SD (n = 3).

Supplemental Figure 6

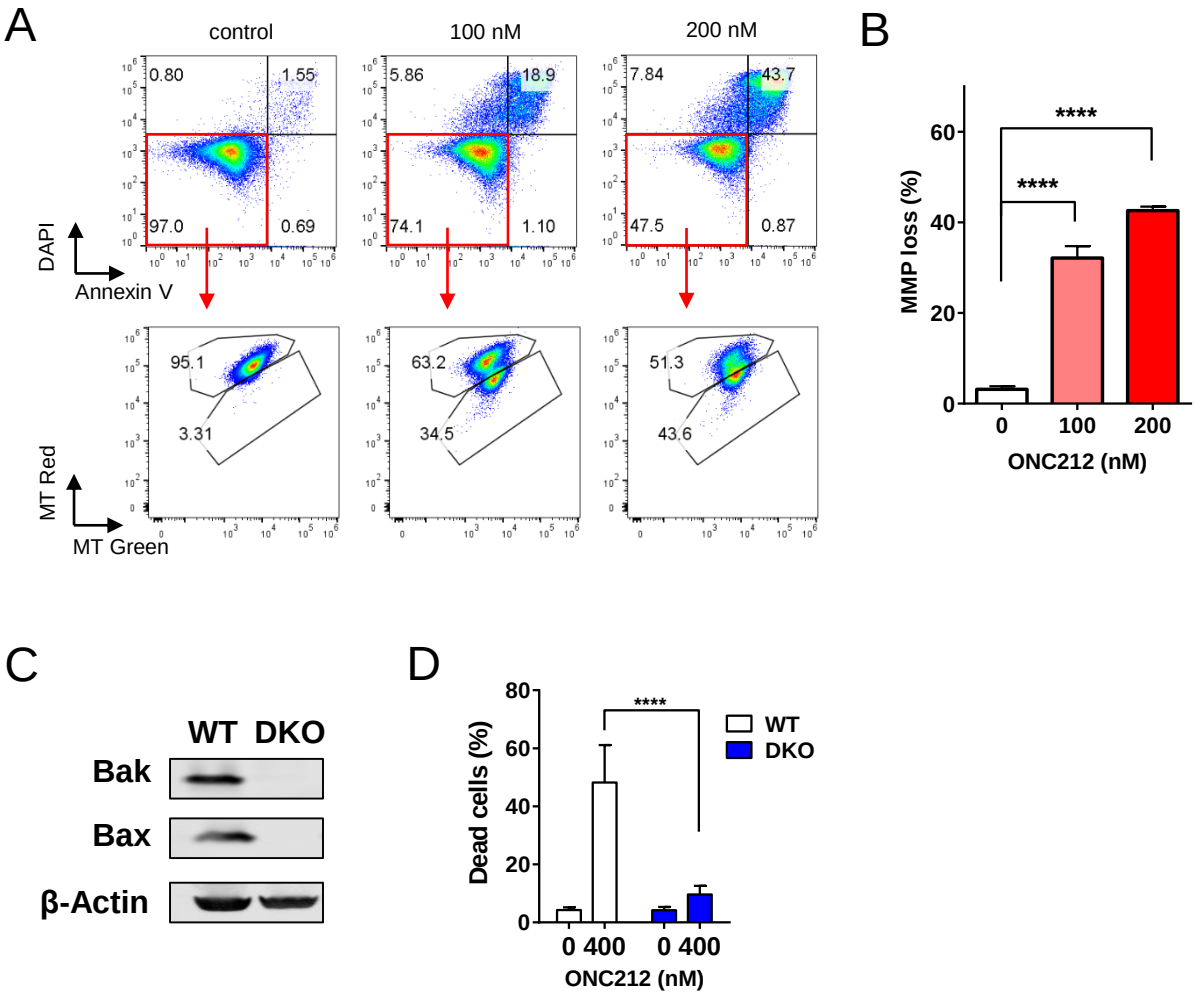

Supplemental Figure 7. ONC212 induces mitochondrial apoptosis.
Representative data of mitochondrial membrane potential (MMP) loss induced by ONC212 72 h treatment (A) and quantification data (B). (C) Western blotting analysis of Bak and Bax expression of wild tipe (WT) and Bak and Bax double knock out MEFs (DKO). (D) The percentage of dead cells (trypan blue positive) induced by ONC212 treatment for 72 h in WT or DKO MEFs. Data are shown as the mean ± SD (n = 3).

Supplemental Figure 7

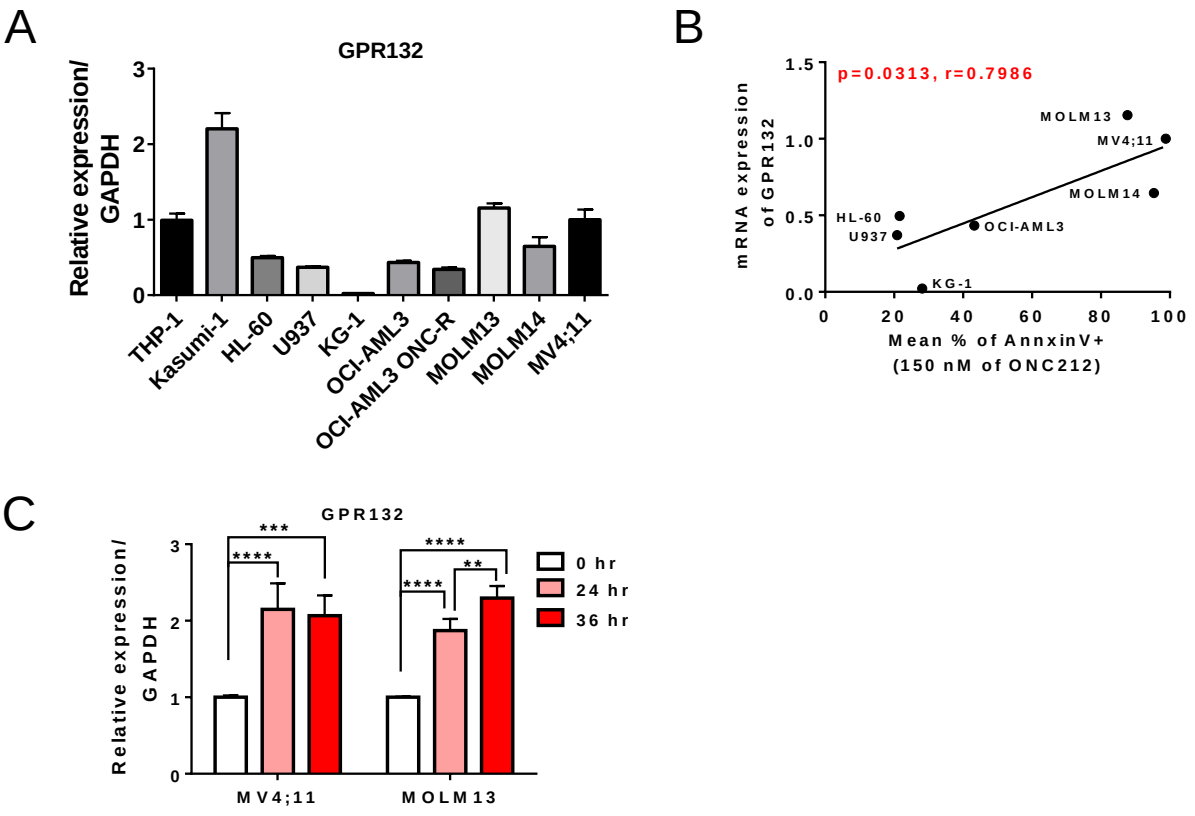

Supplemental Figure 8. ONC212 increases orphan GPCR GPR132 expression. (A) We extract total RNA from indicated AML cell lines and analyzed GPR132 expression by qRT-PCR. GAPDH was used as an internal control. The range given for these genes relative to control were determined by evaluating the expression: 2–ΔΔCT with ΔΔCT + s and ΔΔCT – s, where s = the standard deviation of the ΔΔCT value. (B) Correlation between GPR132 expression and ONC212 effects in AML cell lines, except for THP-1 and Kasumi-1. (C) GPR132 expression after ONC212 treatment. We analyzed the GPR132 expression by qRT-PCR. ONC212 treatment transcriptionally increased GPR132 expression. The ranges given for the gene expression relative to control were determined by evaluating the expression: 2–ΔΔCT with ΔΔCT + s and ΔΔCT – s, where s = the standard deviation of the ΔΔCT value. **; $p < 0.01$, ***; $p < 0.005$, ****; $p < 0.001$.

Supplemental Figure 8

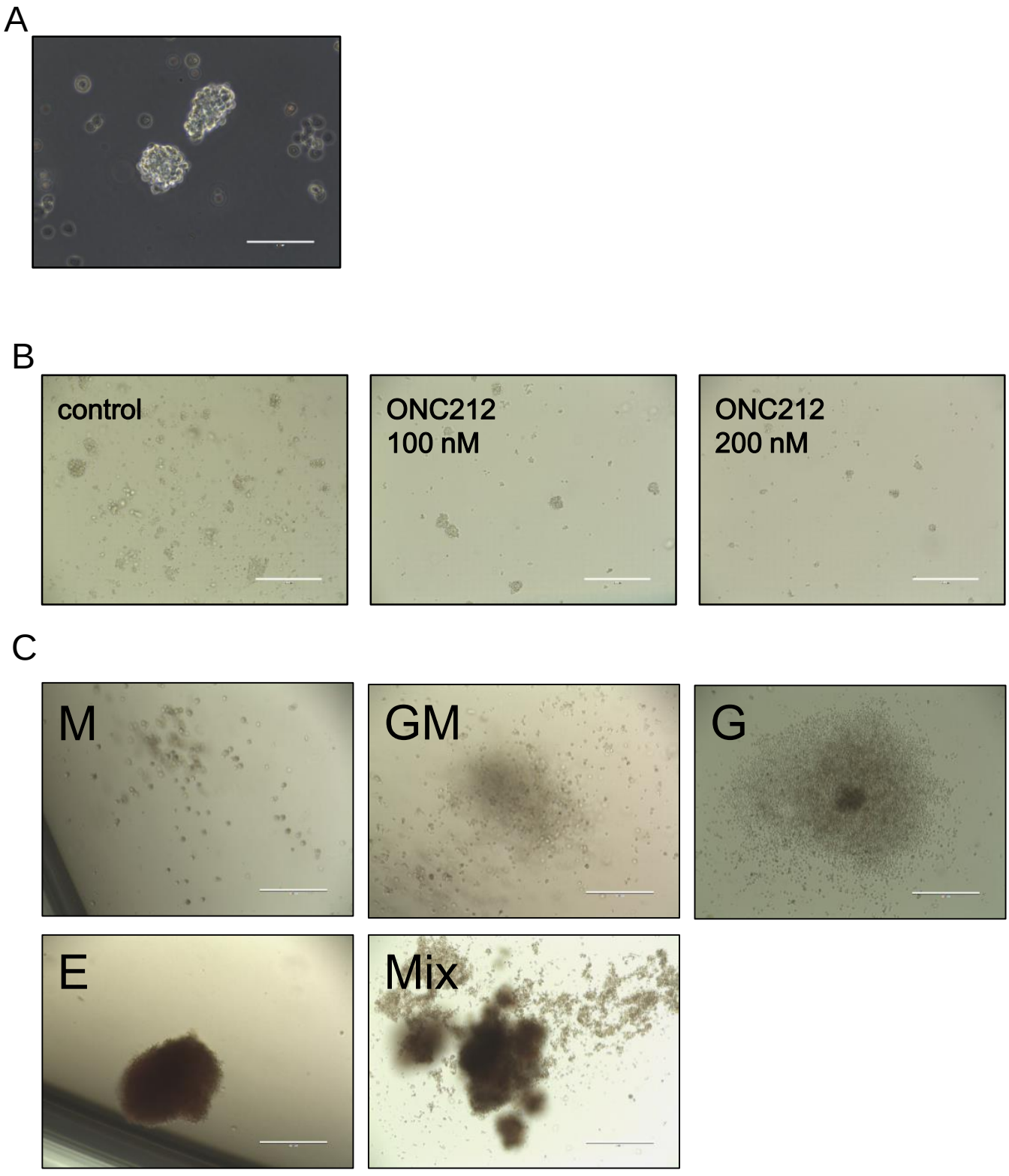

Supplemental Figure 9. ONC212 showed cross resistance with ONC201 in MCL cell lines. (A) Bright-field images of blast colonies derived from patint-1. (B) Bright-field images of blast colonies treated with DMSO (control) or ONC212 (100 or 200 nM). (C) Bright-field images of hematopoietic colonies. M: macrophage, GM: granulocyte and macrophage, G: granulocyte, E: erythroid, Mix: granulocyte erythrocyte macrophage megakaryocyte.

Supplemental Figure 9

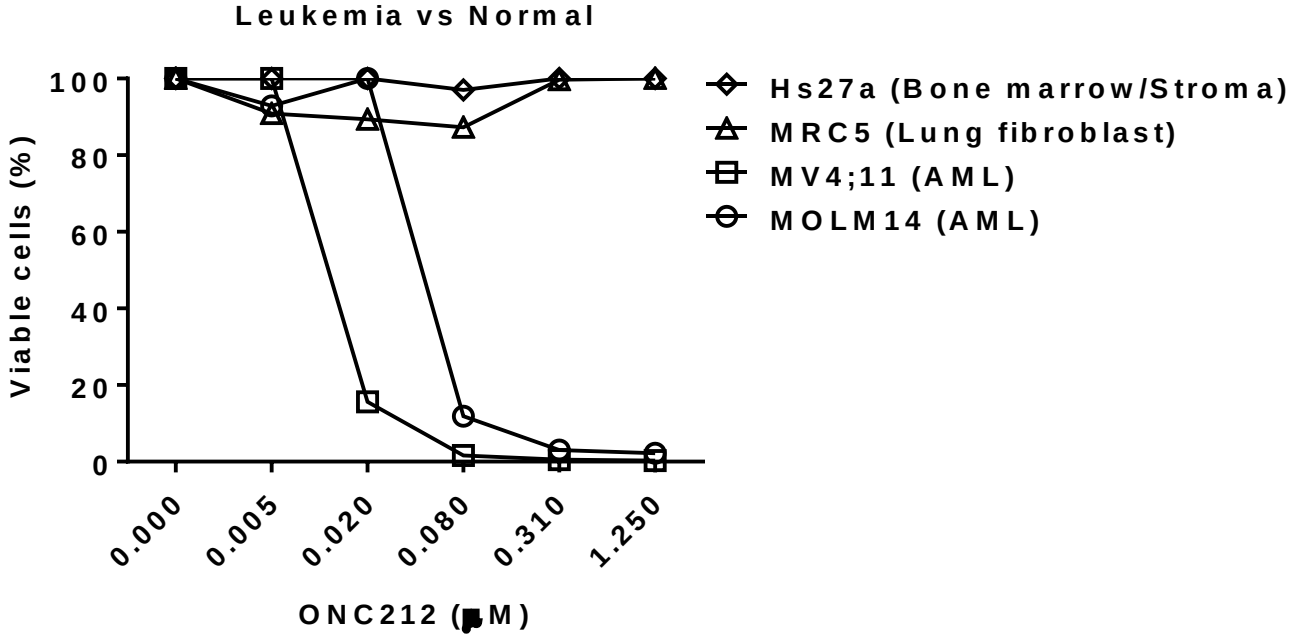

Supplemental Figure 10. Cell viability of MOLM14, MV4;11 AML cell lines, MRC5 lung fibroblasts and Hs27a bone marrow cells treated with ONC212 (5 nM – 5 µM, 72 hr, n=3).

Supplemental Figure 10

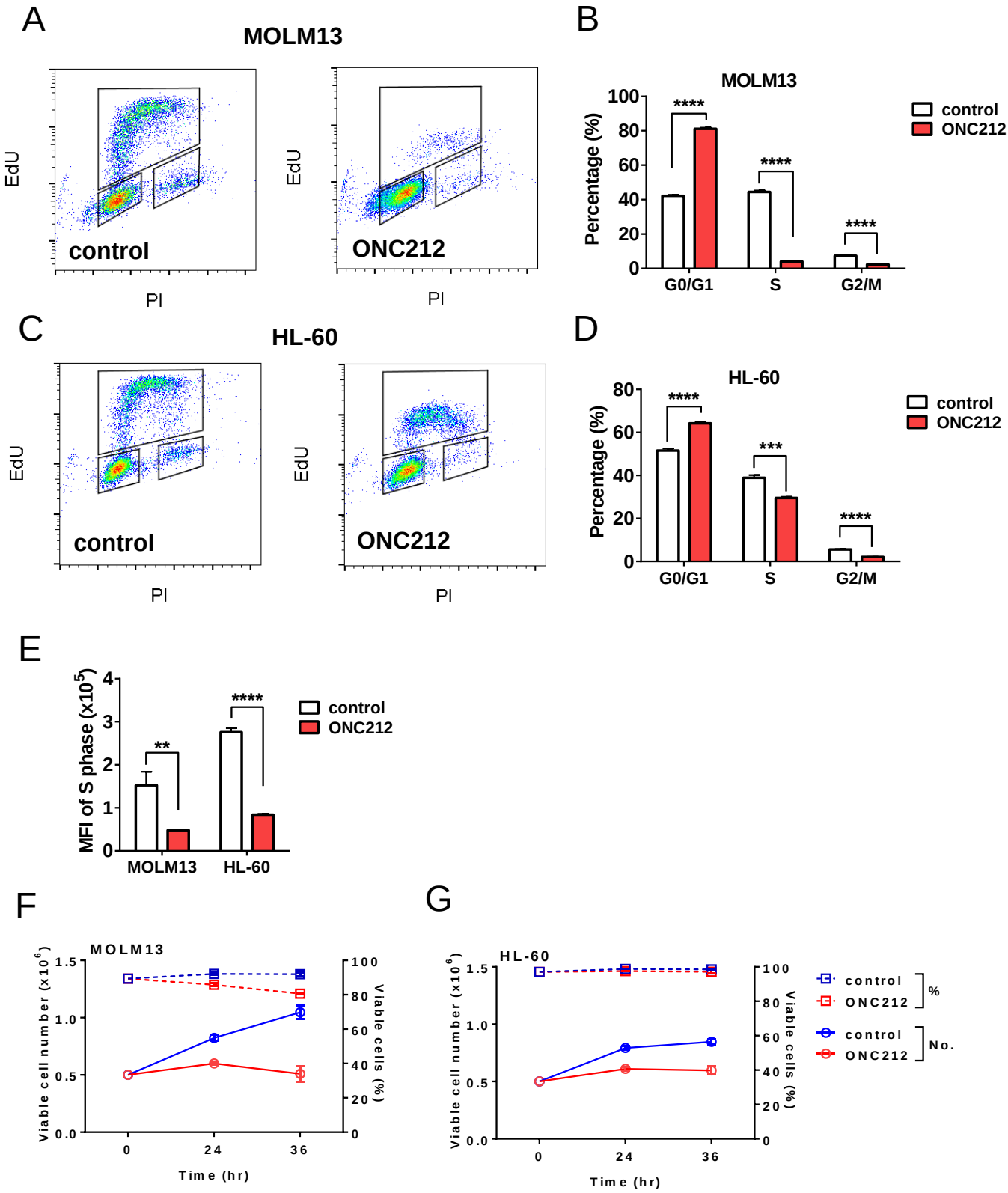

Supplemental Figure 11. ONC212 induced G1/S arrest in AML cell lines. (A-E) Flow cytometric analysis of EdU incorporation combined with DNA content analysis with PI staining in MOLM13 and HL-60. Representative (A and C) and quantification (B and D) data of each cell cycle percentage. (E) Mean fluorescent intensify (MFI) of S-phase. (F and G) The number and percentage of viable MOLM13 and HL-60 treated with or without ONC212 (250 nM). We detected the viable cells by Trypan blue staining. Dotted lines show percentage of viable cells. Solid lines show number of viable cells.

Supplemental Figure 11

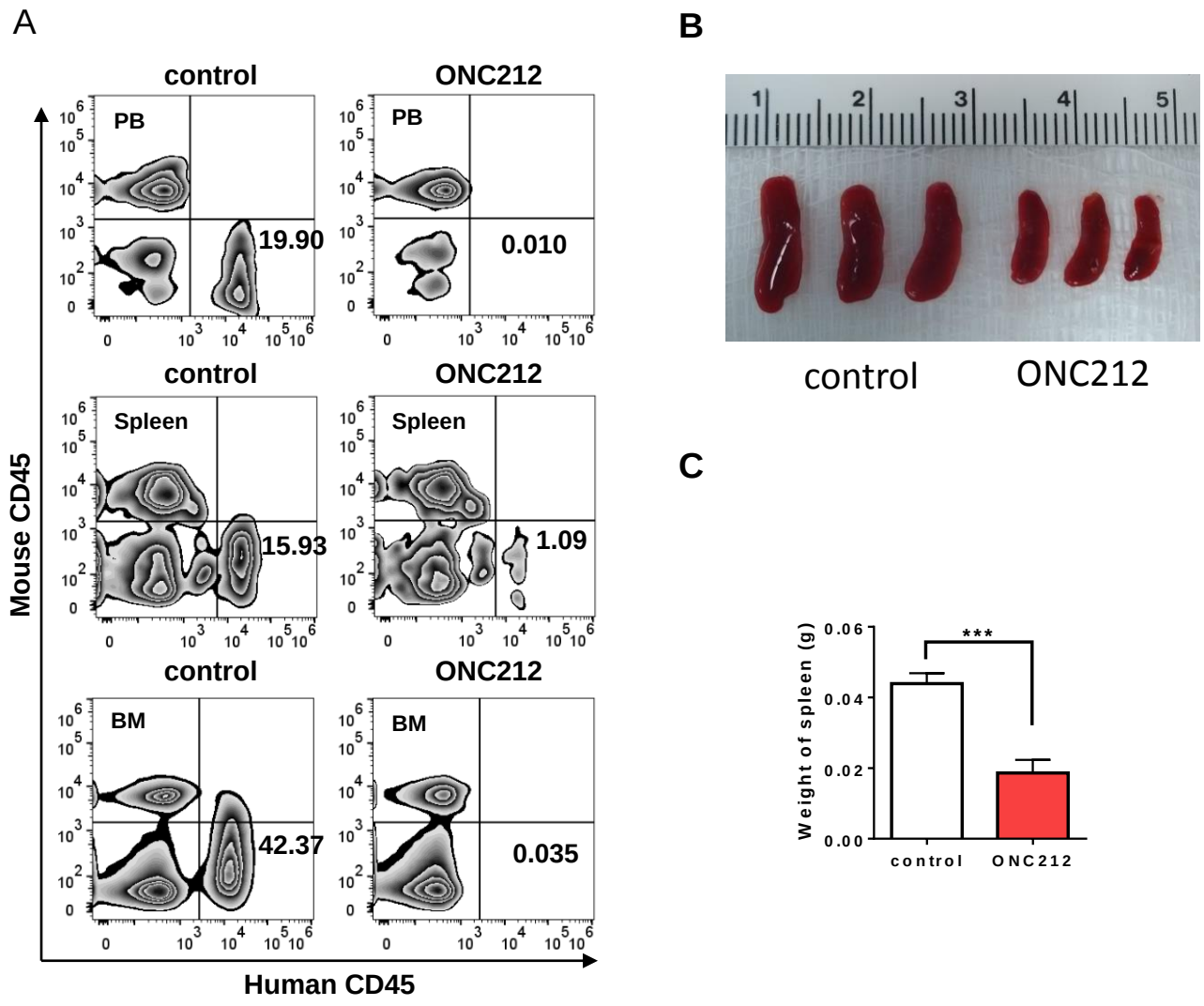

Supplemental Figure 12. Ex vivo treatment of ONC212 inhibits leukemia stem and progenitor cells. One month post-injection of pdx-AML cells with or without ONC212 (250 nM) treatment, we analyzed mouse and human CD45+ cells in peripheral blood (PB), spleen, and BM. (A) Representative data of mouse and human CD45+ cells. Data are shown as the mean (n = 3). Picture (B) and quantification data (C) of spleen size from mice injected pdx-AML with or without ONC212 treatment. Ex vivo ONC212 treatment considerable suppressed the enlargement of the spleen. Data are shown as the mean ± SD (n = 3). ***; $p < 0.005$.

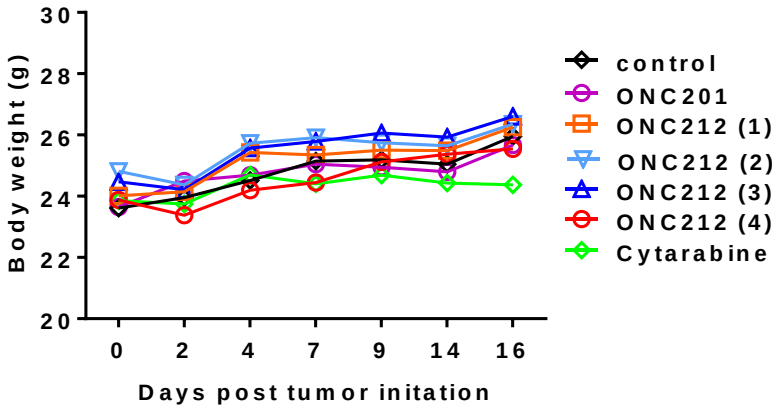

Supplemental Figure 13. *In vivo* efficacy of ONC212 in leukemia xenograft. (A and B) Body weight of AML xenograft model, MV4;11 cells were subcutaneously implanted in the flanks of athymic nude mice, treated with ONC201 (50 mg/kg,/wk), ONC212 [(1) 5 mg/kg/wk; (2) 5 mg/kg, twice/wk; (3) 25 mg/kg, twice/wk; (4) 50 mg/kg/wk] and cytarabine (100 mg/kg, 5 times/wk) (n = 10).

Supplemental Figure 13

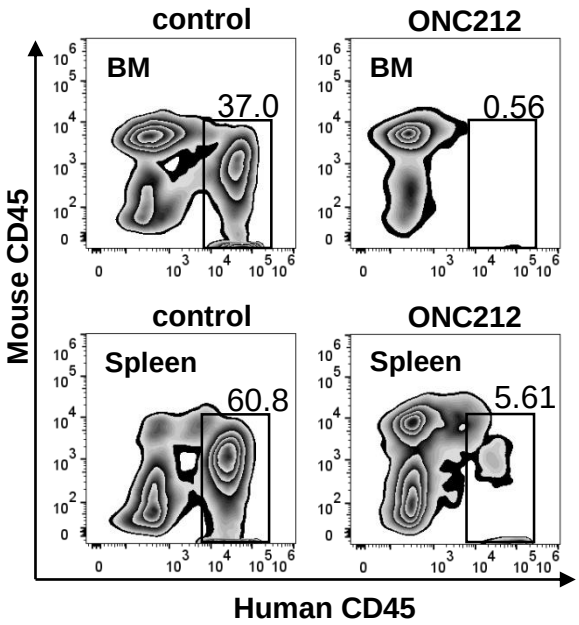

Supplemental Figure 14. Effects of ONC212 on AML propagation *in vivo*. The percentage of mouse and human CD45+ cells in spleen and BM after 45 d of OCI-AML3-Luc cells injection.

Supplemental Figure 14

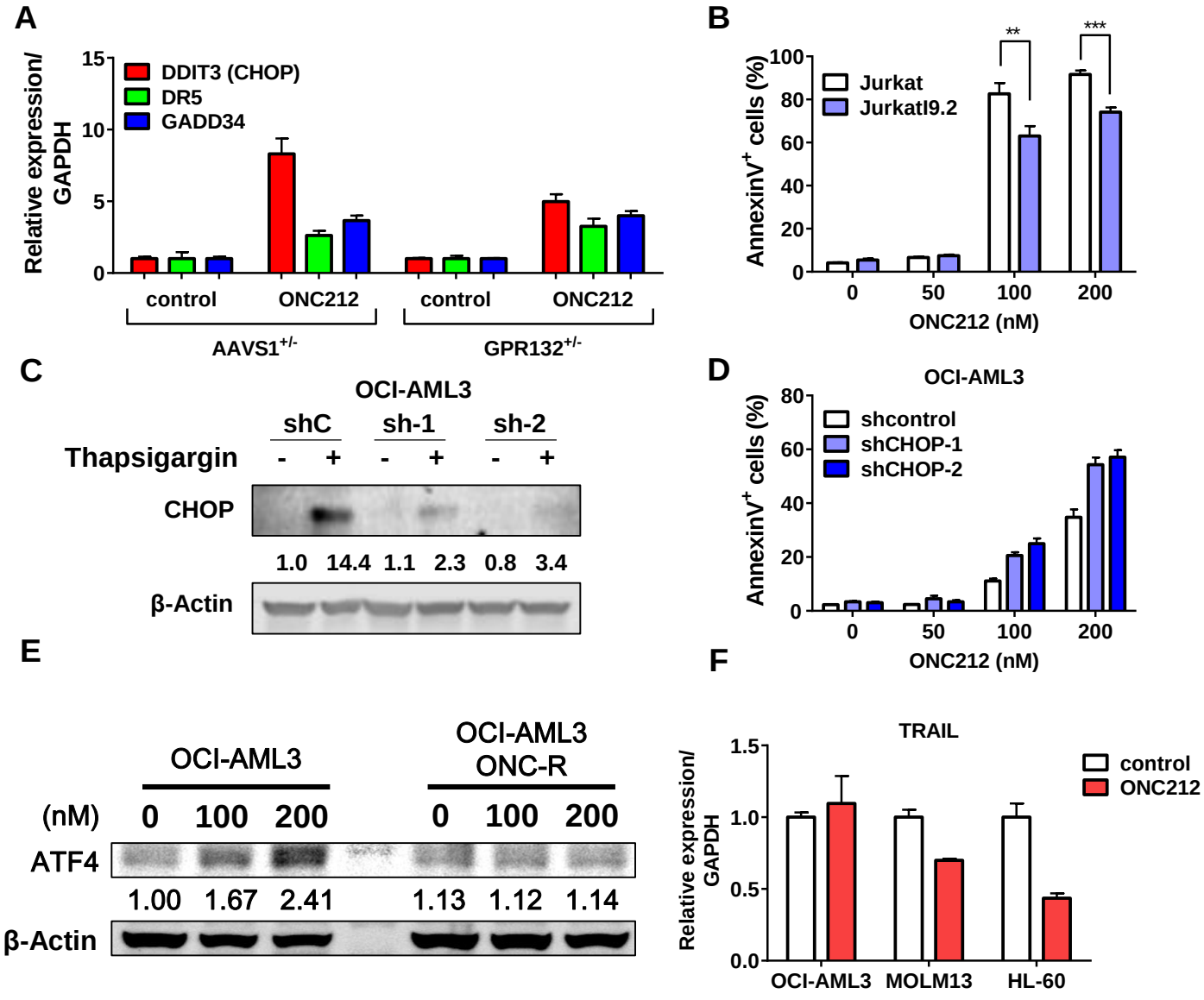

Supplemental Figure 15. ISR related genes expression was upregulated in GPR132 heterozygous knock-out HCT-116.

(A) Relative expression level of CHOP, DR5 amd GADD34. We treated AAVS1 and GPR132 HCT-116 cell lines with or without ONC212 (200 nM) for 48 h and analyzed RNA levels by qRT-PCR. (B) The percentage of apoptotic cells induced by ONC212 treatment for 72 h in Jurkat and JurkatI9.2 cell lines. (C) Western blotting analysis of CHOP expression. We treated OCI-AML3 shRNA control (shC), shRNA-1 (sh-1), and sh-2 cell lines with or without Thapsigargin (1 μM) for 6 h. (D) The percentage of apoptotic cells induced by ONC212 treatment for 72 h inOCI-AML3 shC, sh-1, and sh-2 cell lines. cell lines. (E) Western blotting analysis of ATF4 expression. We treated OCI-AML3 and OCI-AML3 ONC-R with or without ONC212 (100, 200 nM) for 24 h. (F) Relative expression level of TRAIL. We treated OCI-AML3, MOLM13 and HL-60 with or without ONC212 (250 nM) for 24 h and analyzed RNA levels by qRT-PCR. The range given for these genes relative to control were determined by evaluating the expression: 2–ΔΔCT with ΔΔCT + s and ΔΔCT – s, where s = the standard deviation of the ΔΔCT value.

Supplemental Figure 15

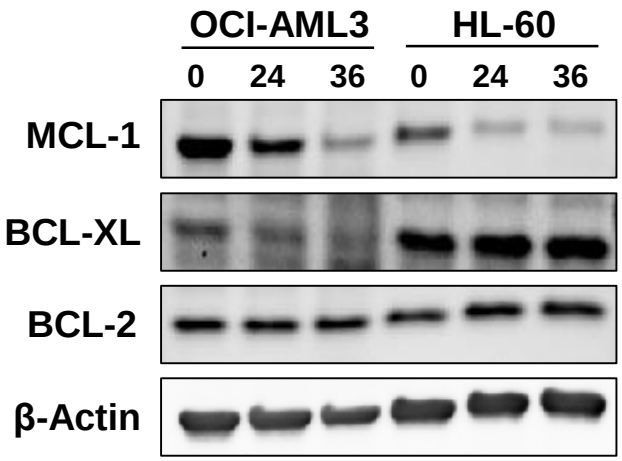

Supplemental Figure 16. Effects of ONC212 on anti-apoptotic BCL-2 family protein. Expression of anti-apoptotic BCL-2 family protein in ONC212-treated AML cell lines**.**

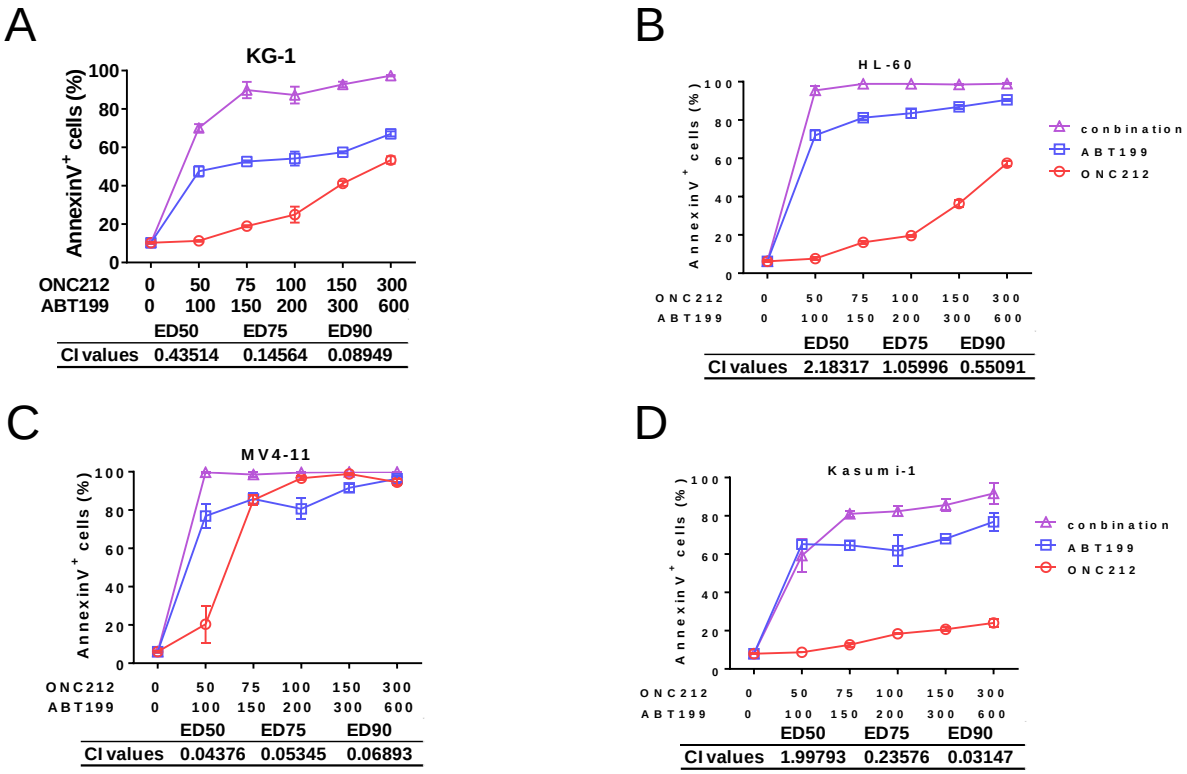

Supplemental Figure 17. Synergistic effects on apoptosis of several AML cell lines by combination of Nutlin-3a or ABT-199 with ONC212.

(A-D) The percentage of annexinV+ cells induced by ONC212 and/or ABT-199. All data are shown as the mean ± SD (n = 3).

Supplemental Figure 17

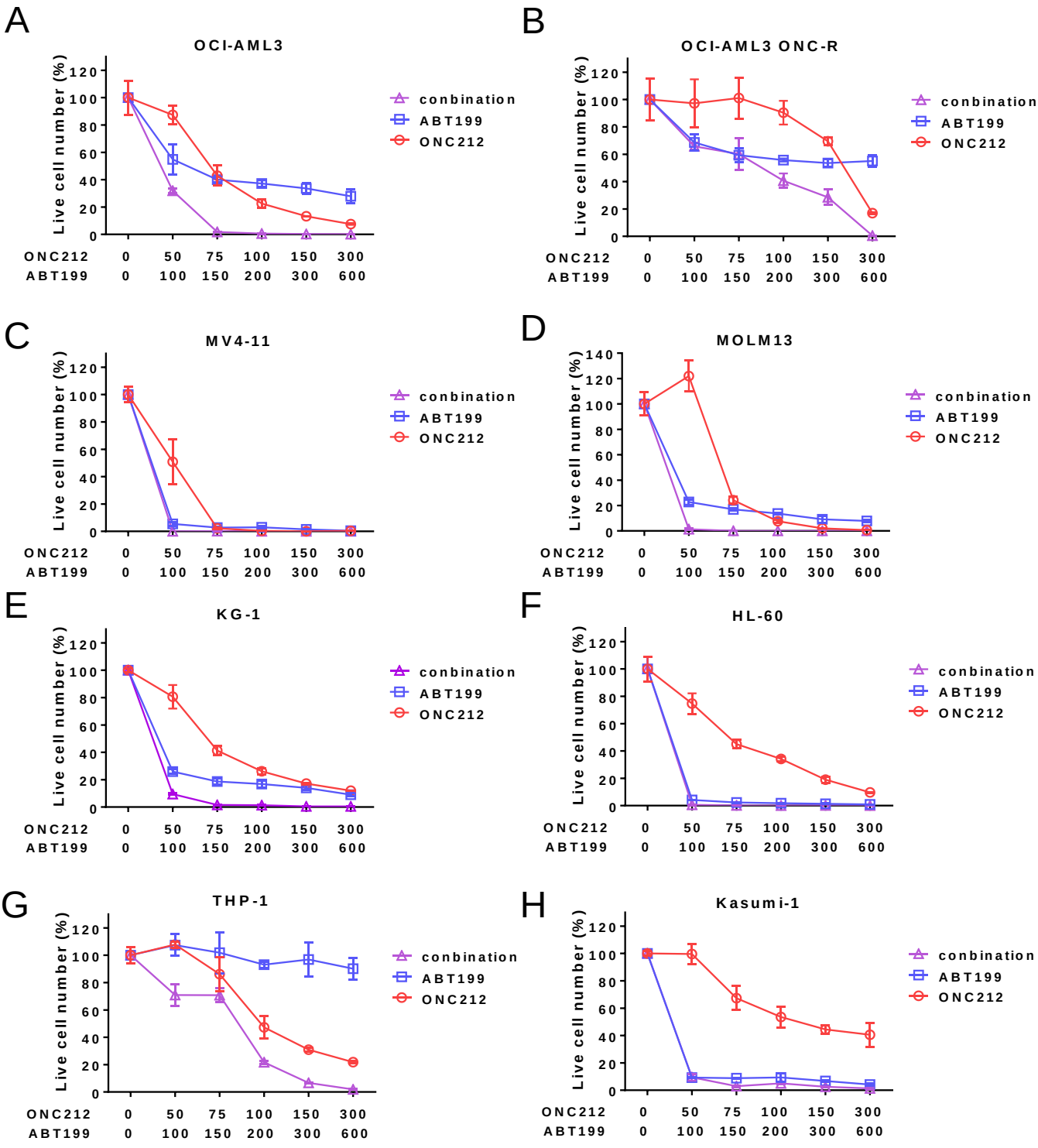

Supplemental Figure 18. Synergistic effects on apoptosis of several AML cell lines by combination of ABT-199 and ONC212. (A-H) The percentage of live cell number treated with ONC212 and/or ABT-199. Data are shown as the mean ± SD (n = 3).

Supplemental Figure 18